

Identification of new diterpene esters from green Arabica coffee beans, and their platelet aggregation accelerating activities

Xia Wang^{a,b,1}, QianQian Meng^{a,1}, XingRong Peng^a, GuiLin Hu^{a,b}, MingHua Qiu^{a,b,*}

^a State Key Laboratory of Phytochemistry and Plant Resources in West China, Kunming Institute of Botany, Chinese Academy of Sciences, Kunming 650201, People's Republic of China

^b University of the Chinese Academy of Sciences, Beijing 100049, People's Republic of China

ARTICLE INFO

Keywords:

Coffea arabica
Coffee lipids
Diterpene esters
Structure elucidation
Platelet aggregation

ABSTRACT

Eight new *ent*-kaurane diterpene fatty acid esters, namely caffarolides A–H (1–8), were isolated from green beans of *Coffea arabica*. Their chemical structures were confirmed by extensive spectroscopic analysis including 1D, 2D NMR (HSQC, HMBC, ¹H–¹H COSY, and ROESY), HRMS, IR and CD spectra and by GC-FID analysis. Interestingly, the diterpene moiety of these new compounds first occurred in genus *Coffea*. All the isolates were evaluated for platelet aggregation activity *in vitro*. As the results, caffarolides C, D and F (3, 4 and 6) showed induction effect for platelet aggregation and the possible structure-activity relationships have been discussed briefly.

1. Introduction

Coffea arabica (Arabica coffee) is the most economic importance specie around 120 species of the genus *Coffea* (Rubiaceae), occupying 61% of the world's coffee production (ICO, 2018). Coffee is one of the most consumed beverages worldwide which is prepared by the ripe seeds from the coffee plants. Chemical investigations showed that coffee is rich in bioactive compounds, such as caffeine, trigonelline, chlorogenic acids, phenolic compounds, diterpenes and melanoidins (Ludwig, Clifford, Lean, Ashihara, & Crozier, 2014). They showed the activities of neuroprotective (Machado-Filho et al., 2014), anti-oxidant (Moreira, Nunes, Domingues, & Coimbra, 2012; Zhou, Zhou, & Zeng, 2013), hepatoprotective (Baeza et al., 2015) and anti-cancer (Cavin et al., 2002). Therefore, long-time coffee consumption will improve several related chronic diseases, such as cardiovascular diseases (Miranda, Steluti, Fisberg, & Marchioni, 2017; Ranheim and Halvorsen, 2005), liver diseases (Muriel & Arauz, 2010; Saab, Mallam, Ii, & Tong, 2014), cognition disorders (Carman, Dacks, Lane, Shineman, & Fillit, 2014; Nehlig, 2016), cancers (Bohn, Blomhoff, & Paur, 2014; Vitaglione, Fogliano, & Pellegrini, 2012) and diabetes (Chu et al., 2011; Pan, Tung, Yang, Li, & Ho, 2016).

The chemical constituents of coffee brews are directly impacted by the chemical compositions of green coffee beans, because green coffee beans contain all the active components (or their precursors) that existed in coffee brews. However, the studies that characterized the chemical compositions of green coffee beans mainly focused on water-soluble fraction (Chu et al., 2016; Shu et al., 2014), but a few on the lipid fraction, despite that the lipid content of green Arabica coffee beans reached 15% (Kurzrock & Speer, 2001).

The main compositions of coffee lipid consist of triacylglycerols, diterpene esters, sterols, sterol esters, and free diterpenes (Durán, Filho, & Maciel, 2010; Kurzrock & Speer, 2001; Speer and Speer, 2006). Among them, cafestol and kahweol are the well-known diterpenes in coffee with cholesterol-raising (Urgert et al., 1995) and anti-cancers (Cavin et al., 2002). However, diterpenes in coffee are rarely present in the form of free (0.4% of the coffee lipid), most of them are esterified with different fatty acids (18% of the coffee lipid) (Kurzrock & Speer, 2001). Until now only a few diterpene esters have been reported, including cafestol, kahweol, 16-*O*-methylcafestol and 16-*O*-methylkahweol with fatty acids C₁₆, C₁₈, C_{18:1}, C_{18:2}, C₂₀, and C₂₂ (Speer and Speer, 2006). Cafestol and kahweol palmitate are the main two diterpene esters that have been reported to enhance glutathione S-

Abbreviations: 1D NMR, proton and carbon nuclear magnetic resonance; 2D NMR, two-dimensional nuclear magnetic resonance; HSQC, heteronuclear single quantum coherence; HMBC, heteronuclear multiple bond connectivity; ¹H–¹H COSY, ¹H–¹H homonuclear chemical shift correlated spectroscopy; ROESY, rotating frame nuclear overhauser and exchange spectroscopy; HRMS, high resolution mass spectrometry; IR, infrared spectroscopy; CD, circular dichroism; GC-FID, gas chromatography with flame ionization detector; TLC, thin layer chromatography; P-TLC, preparative thin layer chromatography; CC, column chromatography; MeOH, methanol; PRP, platelet-rich plasma; PPP, platelet-poor plasma; ADP, adenosine diphosphate

* Corresponding author at: State Key Laboratory of Phytochemistry and Plant Resources in West China, Kunming Institute of Botany, Chinese Academy of Sciences, Kunming 650201, People's Republic of China.

E-mail address: mhchiu@mail.kib.ac.cn (M. Qiu).

¹ These authors contributed equally to this article.

<https://doi.org/10.1016/j.foodchem.2018.04.081>

Received 15 January 2018; Received in revised form 10 April 2018; Accepted 20 April 2018

Available online 22 April 2018

0308-8146/ © 2018 Elsevier Ltd. All rights reserved.

transferase (Huber et al., 2010), inhibit angiogenesis (Moeenfarid et al., 2016) and COX-2 (Muhammada et al., 2007) activities. The presence of diterpene esters in coffee brew is influenced by roasting degree and methods of preparation. In general, the content of total diterpene esters in coffee beans decreased with an increase degree of roasting (Kurzrock & Speer, 2001; Speer and Speer, 2006). Meanwhile, the concentrations of total diterpene esters in different coffee brews were in the order boiled coffee > French press coffee > espresso > filtered coffee and instant coffee due to different contact time, grind degree, filter paper and temperature (Moeenfarid, Erny, and Alves, 2016; Ratnayake, Hollywood, O'Grady, & Stavric, 1993).

Recently, several studies found that coffee extracts can inhibit platelet aggregation *in vitro* (Bydlowski, Yunker, Rymaszewski, & Subbiah, 1987; Naito, Yatagai, Maruyama, & Sumi, 2011), which is a key step in the development of thrombosis and other cardiovascular diseases. Further studies demonstrated that these water-soluble compounds like phenolic acids (Natella et al., 2008), pyridinium compounds (Kalaska et al., 2014) may be responsible for the antithrombotic effect of coffee extract, but the effect of coffee lipids on platelet aggregation has been poorly studied.

Therefore, as part of our systematic chemical investigations on *Coffea arabica*, the aims of the study presented here were to isolate and structurally characterize new diterpene esters from coffee lipid fraction and to evaluate their activities of platelet aggregation (Fig. 1).

2. Material and methods

2.1. General

A Jasco P-1020 polarimeter (Jasco, Japan) was used to obtain optical rotations. Ultraviolet spectra were measured by UV-2401 PC spectrophotometers (Shimadzu, Japan). A Bruker Tensor-27 instrument (Bruker, German) was used for recording infrared spectra by using KBr pellets and HRMS data were measured by an API QSTAR Pulsar spectrometer (Waters, UK). The Bruker AM-400, and DRX-600 instruments (Bruker, Zurich, Switzerland) with transcranial magnetic stimulation (TMS) were used to detect ^1H and ^{13}C NMR spectra. Circular dichroism spectra were scanned by a Chirascan spectropolarimeter (Applied Photophysics, UK). Semi-preparative HPLC was performed on an Agilent HP1100 or 1260 series instrument with a UV L-2400 detector (Agilent, USA) and an ZORBAX SB C-18 column (5 μm , 9.4 mm \times 250 mm, wavelength detection at 220 and 290 nm). The analysis of fatty acid methyl esters was accomplished by an Agilent 6890N gas chromatograph (Agilent Technologies, Germany) equipped with FID detector. The green coffee beans were ground into 50–300 mesh powder by YB-2500B grinder (Yunbang, Yongkang, China).

2.2. Chemical and reagents section

TLC detection was performed on TLC plates (200–250 μm thickness, F254 Si gel 60, Qingdao Marine Chemical, Inc., China). The ordinary column chromatographic materials include Lichroprep RP-18

(40–63 μm , Fuji, Japan), Sephadex LH-20 (20–150 μm , Pharmacia, USA) and Silical gel (200–300 mesh, Qingdao Marine Chemical, Inc., China). The industrial-grade methanol, chloroform, ethyl acetate, acetone, petroleum ether were purchased from Tianjing Chemical Reagents Co. (Tianjing, China). The analytical-grade acetonitrile, tetrahydrofuran, hydrochloric acid, sodium hydroxide, methyl palmitate (16:0), methyl linoleate (18:2), methyl oleate (18:1), methyl nonadecadienoate (19:2), and methyl eicosadienoate (20:2) were purchased from Aladdin Industrial Corporation (Shanghai, China).

2.3. Plant material

The green coffee beans of *Coffea arabica* cultivated in Yunnan province (P. R. China), with a subtropical monsoon climate at the location of 22°68' north altitude and 100.94' east longitude, were harvested in June 2014. The material was authenticated by Ming-Hua Qiu, Kunming Institute of Botany, Chinese Academy of Sciences. A specimen was deposited in State Key Laboratory of Phytochemistry and Plant Resources in West China, Kunming Institute of Botany, Chinese Academy of Sciences.

2.4. Extraction and isolation of the lipid fraction of green Arabica coffee beans

The powder of dried coffee green beans (50–300 mesh, 10 kg) was soaked in acetone for four days at room temperature, then the acetone extract was evaporated under reduced pressure. The residue (963 g) was dissolved with CHCl_3 , filtered with a Buchner funnel and recrystallized for removing caffeine. Then, the CHCl_3 layer (63 g) was subjected to Silica gel column chromatography (CC, 20.0 \times 120 cm) and eluted in a step gradient manner with petroleum ether/acetone (20:1, 5:1, 1:1, 0/100, v/v) to yield four fractions (Fr.): Fr. 1 (16 g), Fr. 2 (9 g), Fr. 3 (5 g), and Fr. 4 (30 g).

Fr. 1 (16 g) was then further separated on a RP C-18 (15.0 \times 100 cm) column and eluted in a gradient of MeOH/ H_2O (55 \rightarrow 80%, v/v) to yield three sub-fractions (Fr. 1-1-1-3). Fr. 1-1 (5 g) was subjected to Silica gel CC (5.0 \times 70 cm), eluted with a CHCl_3 /MeOH (80:1 \rightarrow 20:1, v/v) gradient system to afford four minor fractions (Fr. 1-1-1-1-4) on the basis of TLC analysis. Fr. 1-1-2 (205 mg) was separated by preparative thin layer chromatography (P-TLC, eluting with CHCl_3 /MeOH, 30:1, v/v) to gain 7 (14 mg).

Fr. 2 (9 g) was applied to Silica gel CC (5.0 \times 100 cm) and eluted in a gradient of MeOH/ H_2O (50 \rightarrow 75%, v/v) to yield four fractions (Fr. 2-1-2-4). Fr. 2-1 (3 g) was separated by Silica gel CC (5.0 \times 70 cm, eluted with CHCl_3 /MeOH, 40:1, v/v), to afford five minor fractions (Fr. 2-1-1-2-1-5). Fr. 2-1-2 (330 mg) was subjected to chromatography over RP C-18 (2.0 \times 20 cm, eluted with MeOH/ H_2O , 40–60%, v/v) to obtain 2 (10 mg) and 5 (8 mg). Fr. 2-2 (2 g) was chromatographed on a Silica gel column (5.0 \times 50 cm), eluted with CHCl_3 /MeOH (20:1, v/v) to yield four minor fractions (Fr. 2-2-1-2-2-4). Then, Fr. 2-2-3 (400 mg) was separated by P-TLC, eluted with CHCl_3 /MeOH (30:1, v/v) to gain minor fractions, then separated by reverse-phase semi-preparative HPLC ($\text{CH}_3\text{CN}/\text{H}_2\text{O}$: 40 \rightarrow 70%, 30 min, flow rate = 3.0 mL/min, UV 220, 290 nm) to get 3 (11 mg, t_R = 11.5 min), 6 (9 mg, t_R = 14.7 min), and 8 (8 mg, t_R = 23.4 min). Fr. 2-3 (3 g) was separated by use of Sephadex LH-20 (5.0 \times 200 cm, eluted with MeOH, 100%, 2 L) and divided into three fractions (Fr. 2-3-1-2-3-3), then Fr. 2-3-1 (506 mg) was applied to Silica gel CC (2.0 \times 50 cm), eluted with CHCl_3 /MeOH (10:1, v/v) to afford four minor fractions (Fr. 2-3-1-1-2-3-1-4). Then, Fr. 2-3-1-2 (88 mg) was treated by reverse-phase semi-preparative HPLC ($\text{CH}_3\text{CN}/\text{H}_2\text{O}$: 45 \rightarrow 80%, 35 min, flow rate = 3.0 mL/min, UV 220, 290 nm) to get 1 (20 mg, t_R = 15.5 min), 4 (9 mg, t_R = 21.3 min).

2.4.1. Caffarolide A (1)

White amorphous powder, $[\alpha]^{25}_D$ –246.9 (c = 0.1, CHCl_3); UV (CHCl_3) λ_{max} (log ϵ): 239 (1.59), 201(1.04), 193 (1.05) nm; IR (KBr)

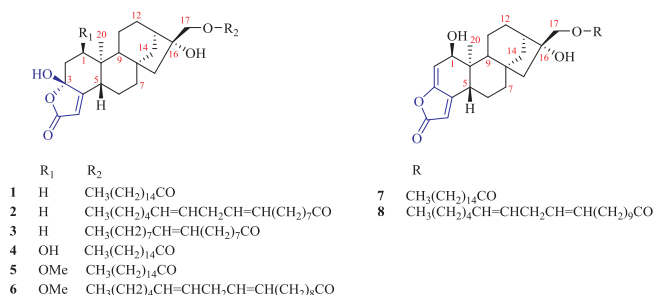


Fig. 1. Structures of diterpene esters isolated from green Arabica coffee beans.

Table 1
¹H NMR Data of Compounds 1–8.^a

Position	1 ^b	1 ^c	2 ^d	3 ^d	4 ^c	5 ^d	6 ^d	7 ^d	8 ^d
1	1.50 (m) 1.77 (m)	1.20 (m) 1.80 (m)	1.50 (m) 1.58 (m)	1.32 (m) 1.88 (m)	3.84 (t, 3.0) –	3.43 s-like –	3.44 s-like –	4.20 (t, 6.0) –	4.20 (t, 6.0) –
2	2.62 (dd, 20.1, 7.6) 1.91 (m)	2.35 (t, 7.3) 2.17 (m)	2.36 (ddd, 14.0, 14.0, 3.0) 1.88 (m)	2.34 (ddd, 14.0, 14.0, 3.0) 1.86 (m)	2.37 (m) 1.94 (m)	2.55 (m) 2.02 (m)	2.55 (m) 1.98 (m)	5.72 (dd, 6.0, 1.5) –	5.72 (dd, 6.0, 1.5) –
5	2.56 (d, 9.0)	2.26 (d, 10.7)	2.34 (m)	2.36 (m)	2.76 (m)	2.67 (m)	2.66 (m)	2.66 (m)	2.69 (m)
6	1.38 (m) 1.53 (m)	1.56 (m) 1.65 (m)	1.49 (m) 1.64 (m)	1.54 (m) 1.67 (m)	1.75 (m) 1.86 (m)	1.63 (m) 1.76 (m)	1.64 (m) 1.76 (m)	1.57 (m) 1.75 (m)	1.58 (m) 1.74 (m)
7	1.54 (m) 1.61 (m)	1.30 (m) 1.61 (m)	1.72 (m) 1.83 (m)	1.64 (m) 1.86 (m)	1.62 (m) 2.23 (m)	1.60 (m) 1.75 (m)	1.61 (m) 1.77 (m)	1.64 (m) 1.88 (m)	1.60 (m) 1.87 (m)
9	1.25 (m)	1.30 (m)	1.29 (m)	1.28 (m)	2.06 (m)	2.01 (m)	2.02 (m)	2.08 (m)	2.08 (m)
11	1.45 (m) 1.91 (m)	1.60 (m) 1.74 (m)	1.65 (m) 1.91 (m)	1.69 (m) 1.94 (m)	1.72 (m) 1.94 (m)	1.53 (m) 1.68 (m)	1.54 (m) 1.78 (m)	1.54 (m) 1.90 (m)	1.47 (m) 1.95 (m)
12	1.50 (m) 1.68 (m)	1.50 (m) 1.59 (m)	1.64 (m) 1.67 (m)	1.53 (m) 1.58 (m)	1.62 (m) 1.66 (m)	1.64 (m) 1.66 (m)	1.54 (m) 1.59 (m)	1.63 (m) 1.66 (m)	1.62 (m) 1.64 (m)
13	2.52 (s)	2.03 (s)	2.34 (m)	2.08 (s)	2.11 (m)	2.18 (s)	2.18 (s)	1.91 (m)	1.89 (m)
14	1.96 (m) 2.05 (m)	1.67 (m) 1.88 (m)	1.74 (m) 1.96 (m)	1.74 (m) 1.96 (m)	1.72 (m) 2.00 (m)	1.68 (m) 1.96 (m)	1.77 (m) 2.00 (m)	1.69 (m) 1.86 (m)	1.68 (m) 1.86 (m)
15	1.65 (m) 1.77 (m)	1.45 (m) 1.68 (m)	1.50 (m) 1.70 (m)	1.58 (m) 1.74 (m)	1.55 (m) 1.77 (m)	1.62 (m) 1.76 (m)	1.62 (m) 1.72 (m)	1.57 (m) 1.75 (m)	1.57 (m) 1.77 (m)
17	4.52 (d, 11.3) 4.68 (d, 11.2)	4.13 (d, 11.4) 4.22 (d, 11.3)	4.23 (d, 13.0) 4.26 (d, 13.0)	4.23 (d, 13.0) 4.26 (d, 13.0)	4.22 (d, 13.0) 4.28 (d, 13.0)	4.22 (d, 13.0) 4.30 (d, 13.0)	4.23 (d, 13.0) 4.30 (d, 13.0)	4.16 (d, 13.0) 4.18 (d, 13.0)	4.16 (d, 13.0) 4.18 (d, 13.0)
18	5.80 (s)	5.78 (s)	5.62 (s)	5.63 (s)	5.72 (s)	5.63 (s)	5.63 (s)	5.76 (s)	5.76 (s)
20	0.75 (s)	0.83 (s)	0.85 (s)	0.86 (s)	0.88 (s)	0.86 (s)	0.86 (s)	0.88 (s)	0.88 (s)
OH-3	–	7.31 (s)	–	–	–	–	–	–	–
OH-16	–	4.43 (s)	–	–	–	–	–	–	–
OMe-1	–	–	–	–	–	3.43 (overlapped)	3.44 (s)	–	–
2'-8'	1.20–1.25 (m)	1.21–1.30 (m)	1.28 (m)	1.28 (m)	1.30 (m)	1.28 (m)	1.30 (m)	1.20 (m)	1.20 (m)
9'	–	–	5.35 (m)	5.35 (m)	–	–	–	–	–
10'	–	–	–	–	–	–	5.34 (m)	–	–
11	–	–	2.77 (m)	1.28 (m)	–	–	–	–	5.33 (m)
12'	–	–	5.35 (m)	–	–	–	2.76 (m)	–	–
13'	–	–	–	–	–	–	5.34 (m)	–	2.77 (m)
14'	–	–	1.28 (m)	–	–	–	–	–	5.33 (m)
15'	–	–	–	–	–	–	1.30 (m)	–	–
16'	0.82 (t, 6.8)	0.91 (t, 6.6)	–	–	0.91 (t, 7.0)	0.86 (t, 7.0)	–	0.78 (t, 7.0)	1.20 (m)
17'	–	–	–	–	–	–	–	–	–
18'	–	–	0.89 (t, 7.0)	0.89 (t, 7.0)	–	–	–	–	–
19'	–	–	–	–	–	–	0.90 (t, 7.0)	–	–
20'	–	–	–	–	–	–	–	–	0.78 (t, 7.0)

^a δ in parts per million, J in Hz, and obtained at 600 Hz. NMR solvent was ^bC₅D₅N, ^cDMSO, ^dCDCl₃, ^eMeOD.

ν_{\max} : 3511, 3422, 3088, 3922, 1767, 1719, 1654, 1453, 1293, 1161, 943, 875 cm⁻¹; HREIMS m/z 586.4225 [M]⁺ (calcd for C₃₆H₅₈O₆, 586.4205); 1D NMR data shown in Tables 1 and 2.

2.4.2. Caffarolide B (2)

White amorphous powder, [α]²⁵_D –164.8 (c = 0.1, CHCl₃); UV (CHCl₃) λ_{\max} (log ϵ): 239 (1.63), 218 (1.27), 201 (1.21) nm; IR (KBr) ν_{\max} : 3440, 2926, 2854, 1736, 1654, 1451, 1239, 1066, 1105, 928, 753 cm⁻¹; HREIMS m/z 610.4249 [M]⁺ (calcd for C₃₈H₅₈O₆, 610.4233); 1D NMR data shown in Tables 1 and 2.

2.4.3. Caffarolide C (3)

White amorphous powder, [α]²⁵_D –149.8 (c = 0.1, CHCl₃); UV (CHCl₃) λ_{\max} (log ϵ): 239 (2.43), 207(0.93), 200 (0.96) nm; IR (KBr) ν_{\max} : 3440, 3423, 2954, 2925, 2853, 1767, 1720, 1629, 1454, 1378, 1342, 1293, 1242, 1162, 1107, 927, 618 cm⁻¹; HREIMS m/z 612.4384 [M]⁺ (calcd for C₃₈H₆₀O₆, 612.4390); 1D NMR data shown in Tables 1 and 2.

2.4.4. Caffarolide D (4)

White amorphous powder, [α]²⁵_D –67.8 (c = 0.1, CHCl₃); UV (CHCl₃) λ_{\max} (log ϵ): 275 (1.05), 238 (1.12), 217 (0.97) nm; IR (KBr) ν_{\max} : 3441, 3424, 2956, 1735, 1630, 1378, 1127, 620 cm⁻¹; HREIMS m/z 602.4201 [M]⁺ (calcd for C₃₆H₅₈O₇, 602.4183); 1D NMR data

shown in Tables 1 and 2.

2.4.5. Caffarolide E (5)

White amorphous powder, [α]²⁵_D –155.4 (c = 0.1, CHCl₃); UV (CHCl₃) λ_{\max} (log ϵ): 239 (1.26), 217 (0.98) nm; IR (KBr) ν_{\max} : 3516, 3451, 2919, 2850, 1748, 1650, 1388, 1239, 1160, 928 cm⁻¹; HREIMS m/z 616.4170 [M]⁺ (calcd for C₃₇H₆₀O₇, 616.4186); 1D NMR data shown in Tables 1 and 2.

2.4.6. Caffarolide F (6)

White amorphous powder, [α]²⁰_D –248.0 (c = 0.1, CHCl₃); UV (CHCl₃) λ_{\max} (log ϵ): 240.4 (2.28) nm; IR (KBr) ν_{\max} : 3485, 3398, 2964, 1721, 1651, 1370, 1240, 1032, 826 cm⁻¹; HRESIMS m/z 677.9326 [M + Na]⁺ (calcd for C₄₀H₆₂O₇, 654.4506); 1D NMR data shown in Tables 1 and 2.

2.4.7. Caffarolide G (7)

White amorphous powder, [α]²⁵_D –138.5 (c = 0.1, CHCl₃); UV (CHCl₃) λ_{\max} (log ϵ): 270 (2.34), 232 (2.18) nm; IR (KBr) ν_{\max} : 3497, 3108, 2922, 1741, 1612, 1390, 1297, 1177, 1089, 983, 873, 566 cm⁻¹; HREIMS m/z 584.4068 [M]⁺ (calcd for C₃₆H₅₆O₆, 584.4077); 1D NMR data shown in Tables 1 and 2.

Table 2
¹³C NMR and DEPT Data of Compounds 1–8.^a

Position	1 ^b	1 ^c	2 ^d	3 ^d	4 ^e	5 ^d	6 ^d	7 ^d	8 ^d
1	35.0 (t)	35.1 (t)	35.6 (t)	35.4 (t)	71.1 (d)	80.4 (d)	80.5 (d)	69.6 (d)	69.6 (d)
2	34.5 (t)	33.8 (t)	34.5 (t)	34.3 (t)	40.9 (t)	35.3 (t)	35.3 (t)	107.1 (d)	106.9 (d)
3	105.5 (s)	104.5 (s)	104.3 (s)	104.1 (s)	107.6 (s)	102.9 (s)	102.8 (s)	152.0 (s)	152.1 (s)
4	173.6 (s)	172.5 (s)	172.4 (s)	172.1 (s)	174.5 (s)	172.7 (s)	172.6 (s)	159.1 (s)	159.0 (s)
5	47.3 (d)	46.4 (d)	47.0 (d)	46.9 (d)	41.3 (d)	40.2 (d)	40.3 (d)	38.7 (d)	38.7 (d)
6	22.0 (t)	21.4 (t)	21.8 (t)	21.5 (t)	22.3 (t)	21.8 (t)	21.6 (t)	21.7 (t)	21.8 (t)
7	40.2 (t)	39.5 (overlapped)	39.5 (t)	39.4 (t)	39.7 (t)	39.0 (t)	39.0 (t)	39.0 (t)	39.0 (t)
8	44.7 (s)	43.9 (s)	44.7 (s)	44.5 (s)	45.6 (s)	44.4 (s)	44.5 (s)	44.3 (s)	44.3 (s)
9	53.6 (d)	52.7 (s)	53.3 (d)	53.2 (d)	45.3 (d)	43.6 (d)	43.6 (d)	46.1 (d)	46.1 (d)
10	43.7 (s)	42.9 (s)	43.7 (s)	43.5 (s)	43.7 (s)	47.5 (s)	47.6 (s)	44.0 (s)	44.0 (s)
11	19.3 (t)	18.6 (t)	19.3 (t)	19.2 (t)	19.5 (t)	18.9 (t)	19.0 (t)	17.8 (t)	19.3 (t)
12	26.3 (t)	25.6 (t)	27.4 (t)	27.2 (t)	27.0 (t)	27.3 (t)	27.4 (t)	25.9 (t)	25.9 (t)
13	46.3 (d)	44.8 (d)	46.0 (d)	45.8 (d)	46.8 (d)	45.9 (d)	45.9 (d)	43.9 (d)	43.9 (d)
14	37.9 (t)	37.1 (t)	37.6 (t)	37.5 (t)	38.3 (t)	37.5 (t)	37.6 (t)	37.1 (t)	37.1 (t)
15	53.9 (t)	52.8 (t)	52.9 (t)	52.7 (t)	54.3 (t)	53.3 (t)	53.3 (t)	53.0 (t)	53.0 (t)
16	79.3 (s)	78.2 (s)	80.2 (s)	80.0 (s)	80.8 (s)	80.0 (s)	80.0 (s)	80.1 (s)	80.1 (s)
17	69.0 (t)	67.1 (t)	68.3 (t)	68.1 (t)	69.3 (t)	68.3 (t)	68.3 (t)	68.3 (t)	68.3 (t)
18	112.5 (d)	111.9 (d)	112.9 (d)	112.8 (d)	113.7 (d)	112.4 (d)	112.4 (d)	112.3 (d)	112.4 (d)
19	171.4 (s)	170.6 (s)	171.1 (s)	170.7 (s)	173.2 (s)	170.8 (s)	170.7 (s)	170.0 (s)	169.8 (s)
20	14.4 (q)	14.0 (q)	14.4 (q)	14.4 (q)	16.0 (q)	15.5 (q)	15.5 (q)	16.0 (q)	16.0 (q)
OMe-1						58.9 (s)	59.0 (s)		
1'	174.0 (s)	173.2 (s)	174.3 (s)	174.1 (s)	176.0 (s)	174.3 (s)	174.2 (s)	174.3 (s)	174.2 (s)
2'	32.1 (t)	31.2 (t)	34.2 (t)	34.0 (t)	31.7 (t)	32.1 (t)	31.7 (t)	34.5 (t)	31.7 (t)
3'-8'	22.9–32.1 (t)	22.4–31.2 (t)	22.8–31.7 (t)	22.5–31.9 (t)	24.5–31.0 (t)	22.9–29.9 (t)	22.7–29.9 (t)	22.9–32.1 (t)	22.8–29.9 (t)
9'			128.0–130.5 (d)	129.7–130.1 (d)					
10'							128.0–130.4 (d)		
11'			27.4	27.3					128.0–130.4 (d)
12'			128.0–130.5 (d)	22.5–31.9 (t)			27.2		
13'							128.0–130.4 (d)		27.4
14'			22.8–31.7 (t)						128.0–130.4 (d)
15'							22.7–29.9 (t)		
16'	14.3 (q)	13.9 (q)			14.6 (q)	14.2 (q)		14.4 (q)	22.8–29.9 (t)
17'									
18'			14.2 (q)	14.3 (q)					
19'							14.6 (q)		
20'									14.2 (q)

^a δ in parts per million, J in Hz, and obtained at 600 Hz. NMR solvent was ^bC₅D₅N, ^cDMSO, ^dCDCl₃, ^eMeOD.

2.4.8. Caffarolide H (8)

White amorphous powder, $[\alpha]^{20}_D -113.5$ ($c = 0.1$, CHCl₃); UV (CHCl₃) λ_{\max} (log ϵ): 269.8 (2.02), 239.2 (1.97) nm; IR (KBr) ν_{\max} : 3485, 3398, 2964, 1721, 1651, 1370, 1240, 1032, 826 cm⁻¹; HRESIMS m/z 659.9114 [M + Na]⁺ (calcd for C₄₀H₄₀O₆, 636.4478); 1D NMR data shown in Tables 1 and 2.

2.5. Mild alkaline hydrolysis of compounds 1–8

Caffarolides A–H (1–8, each for 3.0 mg, respectively) were dissolved in 1 mL of methanol–tetrahydrofuran (1:1, v/v) and treated with 0.1 M NaOH (0.5 mL) at room temperature for 2 h (Tamaki et al., 2008). After that, 0.01 M HCl (~5.0 mL) was added to the reaction mixtures for neutralization. In order to obtain the fatty acid esters, the solutions were extracted with ethyl acetate and then evaporated. The residues were purified by Silica gel column chromatography (1.0 × 10 cm) and eluted in a step gradient manner with CHCl₃/MeOH (100:1 → 10:1, v/v). The fatty acid methyl esters were obtained at 80:1 (CHCl₃/MeOH, v/v) fractions.

2.6. GC comparison analysis for the fatty acid of compounds 1–8

HP-5 capillary column (30 m × 0.53 mm, 1.0 μ m) was used in GC. Column temperature was held initially at 60 °C for 1 min, increased by 10 °C/min to 150 °C and held for 5 min, then by 5 °C/min to 250 °C, then by 20 °C/min to 300 °C and held for 7 min. The carrier gas is helium with the flow rate of 1.1 mL/min and the inlet temperature was set at 200 °C. Then, compared the retention time of the fatty acid methyl esters with those of standards, the GC analysis confirmed that 1, 4, 5, 7

esterified with palmitic acid (16:0, $t_R = 23.5$ min) and 2, 3, 6, 8 were esterified with linoleic acid (18:2, $t_R = 29.8$ min), oleic acid (18:1, $t_R = 27.1$ min), nonadecadienoic acid (19:2, $t_R = 30.2$ min), eicosadienoic acid (20:2, $t_R = 31.7$ min), respectively (Zhao et al., 2014).

2.7. Platelet aggregation assays

2.7.1. Preparation of platelets

blood samples from the rabbit ear central artery (Japanese big ear rabbits, Kunming Chu Shang technology co. Ltd., China) were collected into plastic tubes, anticoagulated with 3.8% sodium citrate acid (9:1, v/v). Platelet-rich plasma (PRP) and platelet-poor plasma (PPP) were obtained by centrifuging the blood at 200 × g (10 min) and 2400 × g (20 min), respectively. Then, cell counter was adjusted to 5 × 10⁸ mL⁻¹ before the measurement (Shen et al., 2003).

2.7.2. Platelet aggregation in vitro

platelet aggregation in PRP was measured as by turbidimetry method (Born, 1964). Firstly, ten disposable cuvettes were prepared. 250 μ L PRP and 2.5 μ L DMSO were added to each cuvette, similarly, another cuvette with 250 μ L PPP and 2.5 μ L DMSO was prepared to adjust baseline of aggregometer. Then, all the cuvettes incubated at 37 °C for 5 min. After incubation, eight new compounds (each 3 × 10⁻⁴ g/mL) and positive control ADP (4.3 × 10⁻⁶ g/mL, Chrono-log Corporation, USA) were added to PRP cuvettes, respectively. Finally, the maximal aggregation was monitored by a chrono-log 700 aggregometer (Chrono-log Corporation, USA).

Every sample was analyzed five times, and data are reported as the mean ± standard deviation expressed as platelet maximum

aggregation rate (%). *P* values < 0.05 were considered significant, < 0.01 highly significant, and < 0.001 extremely significant.

3. Result and discussion

3.1. Phytochemical investigation

Caffarolide A (**1**) was isolated as white amorphous powder, whose molecular formula was determined to be $C_{36}H_{58}O_6$ from the $[M]^+$ ion peaks at m/z 586.4225 (calcd for $C_{36}H_{58}O_6$, 586.4205) in the HREIMS. The IR spectrum indicated that **1** possessed hydroxyl (3422 cm^{-1}), and α,β -unsaturated lactone (1767 cm^{-1}) groups. The ^1H NMR (Table 1) spectrum showed the presence of one singlet methyl (δ_H 0.75, s, H₃-20), one triplet methyl (δ_H 0.82, t, $J = 6.8\text{ Hz}$, H₃-16'), one oxymethylene [δ_H 4.52 (d, $J = 11.2\text{ Hz}$, H-17a), 4.68 (d, $J = 11.3\text{ Hz}$, H-17b)], one olefinic methine (δ_H 5.80, s, H-18), and huge methylene proton signals at δ_H 1.20–1.25 (m, H-2'-15'). The ^{13}C -DEPT spectra (Table 2) displayed a total of 36 carbon resonances. Except for the characteristic huge methylenes, one methyl and one ester carbonyl signals for fatty acid, the remaining resonances were assigned to be one methyl, eight methylenes (one oxygenated), four methines (one olefinic), and seven quaternary carbons (including one olefinic, one carbonyl and two oxygenated). The aforementioned information indicated that compound **1** could be a diterpene ester and the diterpene moiety was exactly similar with tricalysiolide B (Nishimura et al., 2006), which was confirmed by the HMBC correlations of δ_H 5.80 (H-18) with δ_C 171.4 (C-19), δ_C 173.6 (C-4), δ_C 105.5 (C-3) and δ_C 47.3 (C-5), of δ_H 4.68 (H₂-17) with δ_C 79.3 (C-16), δ_C 46.3 (C-13) and δ_C 53.9 (C-15) (Fig. 2). Moreover, on the basis of the molecular weight, the fatty acid was determined to be palmitic acid (16:0), which was further confirmed by the alkaline hydrolysis, then, comparing to the retention time of standard methyl palmitate in GC analysis ($t_R = 23.5\text{ min}$) (Novaes, Oigman, Rezende, & Neto, 2015). Additionally, the esterification position was located at C-17, which was proved by the key HMBC correlation of δ_H 4.68 and 4.52 (H₂-17) with δ_C 173.6 (C-1') and δ_C 79.3 (C-16) (Fig. 2).

The relative configuration of **1** was established by ROESY spectrum as shown in Fig. 2. With the solvent of DMSO instead of C_5N_5D (Supporting Information), the ROESY correlations of H-13/H₂-17 and OH-3/H-5 assigned OH-16 and OH-3 as α -orientation and β -orientation, respectively. The absolute configuration at C-3 was established by the CD spectrum (a $\pi-\pi^*$ transition in the α,β -unsaturated- γ -lactone moiety). The observed negative Cotton effect at 225 nm revealed the 3R configuration (Supporting Information), which was supporting by literatures (Shen, Luo, Yang, & Kong, 2015; Yin, Luo & Kong, 2013). Finally, the structure of **1** was established as caffarolide A.

Caffarolide B (**2**) was obtained as white amorphous powder. The molecular formula $C_{38}H_{58}O_6$ was deduced from the molecular ion peak at m/z $[M]^+ 610.4249$ (calcd for $C_{38}H_{58}O_6$, 610.4233) in HREIMS. The NMR spectra of **2** were similar to those of **1** implying that **2** has the same structure as **1** containing a diterpenoid moiety and a fatty acid fraction. Comparison of the ^{13}C -DEPT spectra between **2** and **1** showed

that the diterpenoid moiety of **2** was also tricalysiolide B (Nishimura et al., 2006). Similarly, the molecular weight of **2** suggested the presence of 18-carbon fatty acid in **2**. Furthermore, four additional sp^2 methine carbons (δ_C 128.0–130.5) in **2** combined with the HMBC correlations of these aromatic signals (δ_H 5.35, m) with huge sp^3 methylenes (δ_C 22.0–30.0) of fatty acid (Fig. 2), together with the ^1H - ^1H COSY correlations of H-10'/H-11'/H-12', indicated that the fatty acid of **2** could be linoleic acid (18:2). Subsequently, the hydrolysis experiment and GC comparison unambiguously determined the fatty acid to be linoleic acid (18:2, $t_R = 29.8\text{ min}$). In the HMBC experiment, δ_H 4.22 and 4.27 (H₂-17) showed a correlation with δ_C 174.3 (C-1') demonstrated the esterification position of **2** was at C-17. The relative configuration of **2** was the same as that of **1** by the ROESY and CD spectra. Then, the structure of **2** was established and named as caffarolide B.

The HREIMS data for caffarolide C (**3**) indicated a molecular formula of $C_{38}H_{60}O_6$, with two units more than **2**. Detailed analysis of the 1D NMR data of **3** and **2** revealed that **3** has the same basic diterpene structure as **2**, expect that the fatty acid in **3** possessed only one double bond. We thus deduced that the fatty acid of **3** could be oleic acid (18:1). The further evidence was established by the HMBC correlation of the H₂- sp^2 methine signals (δ_H 5.34, m) with huge sp^3 methylenes (δ_C 22.5–31.9) of fatty acid, along with GC comparison analysis ($t_R = 27.1\text{ min}$). Moreover, the esterification location of **3** was at C-17, according to the key HMBC correlation of with C-1'. Its relative configuration was determined to be the same as that of **1** from the ROESY and CD spectra. Therefore, the structure of **3** was determined.

On the basis of HREIMS spectrum, caffarolide D (**4**) was assigned a molecular formula of $C_{36}H_{58}O_7$. The 1D NMR data of **4** were similar to those of **1** with a palmitoyl group, except that the methylene at C-1 in **1** was replaced by an oxymethine in **4**. The observed HMBC correlations of the singlet methyl δ_H 0.88 (H₃-20), the methylene proton δ_H 2.37 (H-2a) and methine proton δ_H 2.06 (H-9) with the oxygenated methine δ_C 71.1, of oxymethine δ_H 3.84 (H-1) with C-2 (δ_C 40.9) and C-3 (δ_C 107.6), together with the ^1H - ^1H COSY correlation of H-1/H-2a indicated that a hydroxyl was located at C-1 (Fig. 3). Herein, the planar structure of the cafestol-type lactone moiety in **4** was established. Meanwhile, combined the results of the molecular weight, hydrolysis experiment and GC comparison analysis, the fatty acid of **4** was determined to be palmitic acid (16:0). Furthermore, the esterification position of **4** was located at C-17, which was proved by the key HMBC correlations of δ_H 4.22 and 4.28 (H₂-17) with δ_C 176.0 (C-1'). Its relative configuration was determined to be the same as that of **1**, and the OH-1 group was assigned as β -oriented as indicated by the ROESY correlation of H-1/H-20 (Fig. 3). Finally, the structure of **4** was elucidated as shown.

Caffarolide E (**5**) was assigned a molecular formula of $C_{37}H_{60}O_7$. Compared the 1D NMR data of **5** with those of **4**, showed that a methoxy (δ_C 58.9) at C-1 in **5** replaced the hydroxyl in **4**. The deduction was proved by the key HMBC correlations of the methyl δ_H 0.86 (H₃-20), the methylene proton δ_H 2.55 (H-2a) and methine proton δ_H 2.01 (H-9) with the oxygenated methine δ_C 80.4, of oxymethine δ_H 3.43 (H-1) with C-2 (δ_C 35.3) and C-3 (δ_C 102.9). The fatty acid of **5** was assigned as palmitic acid (16:0) by the molecular weight and GC comparison analysis ($t_R = 23.5\text{ min}$). The esterification location of **5** was also at C-17, which was confirmed by the HMBC spectrum. In the ROESY spectrum of **5**, the correlations of H-1/H-20 assigned OMe-1 as β -orientation. Therefore, the structure of compound **5** was elucidated as shown.

Caffarolide F (**6**) was assigned a molecular formula as $C_{40}H_{62}O_7$ from its HRESIMS spectrum. Analyzed the 1D NMR data of **6** and **5** indicated that **6** has the same diterpene lactone moiety as **5**, but differing at the fatty acid moiety. Four additional sp^2 methine singals were also observed in the downfield region of **6**. Thus, based on the molecular weight, we deduced that the fatty acid of **6** could be nonadecadienoic acid (19:2). The HMBC correlations of these H₄- sp^2 methine signals (δ_H 5.34) with huge sp^3 methylenes (δ_C 22.7–29.9), together with GC

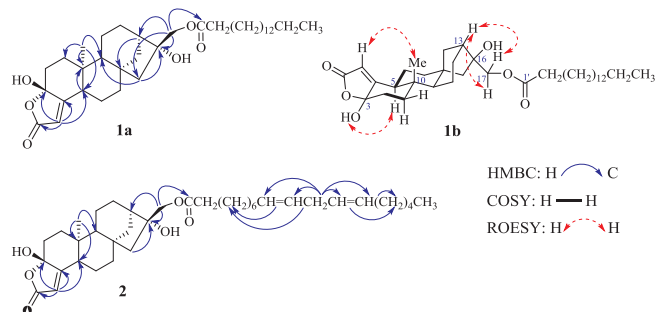


Fig. 2. Key HMBC (H → C) for **1a** and **2**, ^1H - ^1H COSY (—), ROESY (H → H) correlations for **1b**.

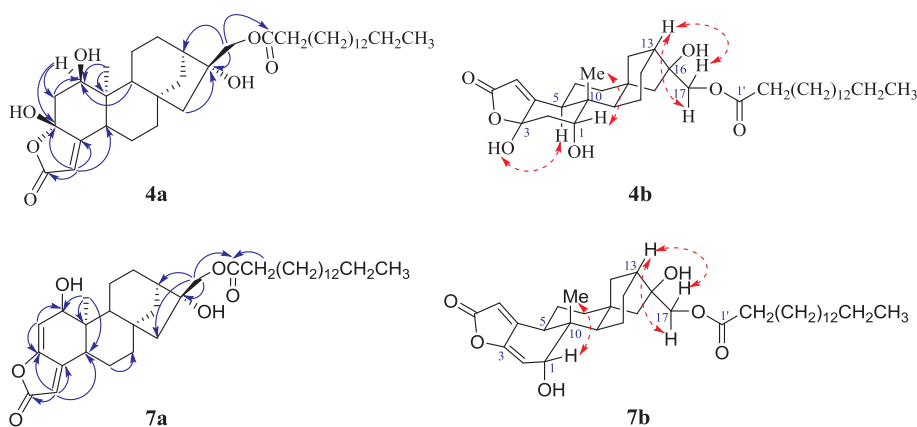


Fig. 3. Key HMBC (H → C) for **4a** and **7a**, ROESY (H ↔ H) correlations for **4b** and **7b**.

comparison analysis ($t_R = 30.2$ min) proved the hypothesis. Moreover, H₂-17 showed the HMBC correlation with C-1', demonstrated that the esterification location of **6** was at C-17. The relative configurations of **6** was determined by the ROESY spectrum, which indicated that OMe-1 were β -orientation. Thus, we deduced the structure of compound **6** as caffarolide F.

For support of the absolute configurations assigned for compounds **2–6**, the CD spectra were measured. The CD spectra obtained were in close agreement with that of **1** at 225 nm, thus indicating that the absolute configuration of C-3 in **2–6** is R, the same as that of **1**.

The HREIMS data for caffarolide G (**7**) indicated a molecular formula of C₃₈H₅₆O₆. The 1D NMR data of **7** were generally similar to those of **4**, but an additional double bond was presented at the diterpene lactone moiety in **7**. The HMBC correlation of H-2 (δ_H 5.72, dd, $J = 6.0$ and 1.5 Hz) with C-1 (δ_C 69.5), C-3 (δ_C 152.0), C-4 (δ_C 159.1), of H-18 (δ_H 5.76) with C-3 (δ_C 152.0) and C-19 (δ_C 170.0), of H-1 (δ_H 4.20, d, $J = 6.0$ Hz) with C-20 (δ_C 16.0), C-2 (δ_C 107.1) and C-3 (δ_C 152.0), together with the ¹H–¹H COSY correlations H-1/H-2 (Fig. 3), demonstrated the double bond was located at C-2 and C-3. Hereto, the planar structure of the diterpene moiety in **7** was determined as tricalysiolide F (Nishimura et al., 2006). Similarly, the fatty acid of **7** was assigned as palmitic acid (16:0) by molecular weight and GC comparison analysis ($t_R = 23.5$ min). C-17 was confirmed as the esterification location of **7** by the HMBC spectrum. The key ROESY correlations of H-1/H-20 and H-13/H₂-17 were assigned OH-1 and OH-16 as β -orientation and α -orientation, respectively (Fig. 3). Therefore, the structure of **7** was determined as caffarolide G.

The molecular formula of caffarolide H (**8**) was assigned to be C₄₀H₄₀O₆. Detailed comparison of 1D NMR data of **8** and **7** showed that the only difference between them was fatty acid fraction. On the basis of the molecular weight, the fatty acid contains twenty carbons. Meanwhile, four *sp*² methine singals were also observed in the down-field region of **8**. Therefore, we assumed the fatty acid of **8** could be eicosadienoic acid (20:2), which was proved by hydrolysis experiment and GC comparison method ($t_R = 31.7$ min). The esterification location of **8** was also at C-17 which was established by the HMBC spectrum. Based on the ROESY spectrum, OH-1 and OH-16 were assigned as β -orientation and α -orientation, respectively. Thus, we deduced the structure of compound **8** as caffarolide H.

3.2. Platelet aggregation assay

The activity of caffarolides A–H (**1–8**) inducing platelet aggregation *in vitro* were evaluated by turbidimetry method, and the results are showed in Table 3. Compared to control (DMSO, $3.4 \pm 1.1\%$), compounds **3**, **4** and **6** showed platelet aggregation activity at the concentration of 3×10^{-4} g/mL, with induction rate of 11.4 ± 5.5 , 15.8 ± 5.6 and $7.8 \pm 3.3\%$, respectively.

From these results, some primary structure-activity relationships

Table 3

Platelet Aggregation Data of Compounds **1–8**.

Compound	Final concentration	Platelet maximum aggregation rate (%)
DMSO (Con.)	1% (v/v)	3.4 ± 1.1
ADP (Pos.)	4.3×10^{-6} g/mL	$53.6 \pm 5.6^{***}$
1	3×10^{-4} g/mL	2.0 ± 1.4
2	3×10^{-4} g/mL	6.8 ± 5.3
3	3×10^{-4} g/mL	$11.4 \pm 5.5^+$
4	3×10^{-4} g/mL	$15.8 \pm 5.6^{**}$
5	3×10^{-4} g/mL	6.0 ± 3.7
6	3×10^{-4} g/mL	$7.8 \pm 3.3^+$
7	3×10^{-4} g/mL	2.4 ± 0.9
8	3×10^{-4} g/mL	2.6 ± 0.9

Results are presented as means \pm standard deviation of quintuple measurements. Different symbols in rows represent significant differences at ⁺ $P < 0.05$, ^{**} $P < 0.01$, ^{***} $P < 0.001$.

can be deduced: the hemiketal at C-3, the substituent groups at C-1 and the types of fatty acids can impact the platelet aggregation effect. If the hemiketal at C-3 in compound **4** was replaced by the enol group in compound **7**, no platelet aggregation effect was shown. When the unsaturated fatty acids were linked to the hydroxyl at C-17, compounds **3** and **6** showed platelet induction activity, whereas, the substitute of saturated fatty acids at C-17, compounds **1** and **5** didn't show any activity. Moreover, the hydroxyl and methoxyl attached to C-1 enhanced the platelet induction activity (**4** vs. **5** vs. **1**).

4. Conclusions

In present study, a systematic chemical research was performed and resulted in the separation of eight new diterpenes esters caffarolides A–H (**1–8**) from the lipid of green Arabica coffee beans. The structures of these new compounds were identified based on detailed spectroscopic analysis (NMR, HSMS, IR and CD spectra) and GC-FID analysis. Caffarolides C, D and F (**3**, **4** and **6**) showed induction effect for platelet aggregation at 3×10^{-4} g/mL. The results obtained in this study complement the current knowledge of diterpene esters in *Coffea arabica*.

Acknowledgements

This research work was supported financially by the National Natural Science Foundation of China (No. 31670364). Project of Key New Productions of Yunnan Province, Centre of CHINA (No. 2015BB002 and No. 2016HE003). The STS Programme of Chinese Academy of Sciences (KFJ-SW-ST-143-8), as well as Foundation of State Key Laboratory of Phytochemistry and Plant Resources in West China (P2015-ZZ09). Furthermore, the authors sincerely thank the support of the analytical center and activity screening center of State

Key Laboratory of Phytochemistry and Plant Resources in West China for the analysis and platelet aggregation activities data.

Notes

The authors declare no competing financial interest.

Appendix A. Supplementary data

Supplementary data associated with this article can be found, in the online version, at <https://doi.org/10.1016/j.foodchem.2018.04.081>.

References

- Baeza, G., Amigo-Benavent, M., Sarriá, B., Goya, L., Mateos, R., & Bravo, L. (2015). Green coffee hydroxycinnamic acids but not caffeine protect human HepG2 cells against oxidative stress. *Food Research International*, 62, 1038–1046.
- Bohn, S. K., Blomhoff, R., & Paur, I. (2014). Coffee and cancer risk, epidemiological evidence, and molecular mechanisms. *Molecular Nutrition & Food Research*, 58(5), 915–930.
- Born, G. V. R. (1964). Strong inhibition by 2-chloroadenosine of the aggregation of blood platelets by adenosine diphosphate. *Nature*, 202, 95–96.
- Bydlowski, S. P., Yunker, R. L., Rymaszewski, Z., & Subbiah, M. T. (1987). Coffee extracts inhibit platelet aggregation in vivo and in vitro. *International Journal for Vitamin & Nutrition Research*, 57, 217–223.
- Carman, A. J., Dacks, P. A., Lane, R. F., Shineman, D. W., & Fillit, H. M. (2014). Current evidence for the use of coffee and caffeine to prevent age-related cognitive decline and Alzheimer's disease. *Journal of Nutrition Health & Aging*, 18, 383–392.
- Cavin, C., Holzhaeuser, D., Scharf, G., Constable, A., Huber, W. W., & Schilter, B. (2002). Cafestol and kahweol, two coffee specific diterpenes with anticarcinogenic activity. *Food and Chemical Toxicology*, 40, 1155–1163.
- Chu, Y. F., Chen, Y., Black, R. M., Brown, P. H., Lyle, B. J., Liu, R. H., & Ou, B. (2011). Type 2 diabetes-related bioactivities of coffee: Assessment of antioxidant activity, NF- κ B inhibition, and stimulation of glucose uptake. *Food Chemistry*, 124, 914–920.
- Chu, R., Wan, L. S., Peng, X. R., Yu, M. Y., Zhang, Z. R., Zhou, L., ... Qiu, M. H. (2016). Characterization of new ent-kaurane diterpenoids of Yunnan arabica coffee beans. *Natural Products and Bioprospecting*, 6, 217–223.
- Durán, M. A., Filho, R. M., & Maciel, M. R. W. (2010). Rate-based modeling approach and simulation for molecular distillation of green coffee oil. *Computer Aided Chemical Engineering*, 28, 259–264.
- Huber, W. W., Teitel, C. H., Coles, B. F., King, R. S., Wiese, F. W., Kaderlik, K. R., ... Ilett, K. F. (2010). Potential chemoprotective effects of the coffee components kahweol and cafestol palmitates via modification of hepatic N-acetyltransferase and glutathione S-transferase activities. *Environmental & Molecular Mutagenesis*, 44, 265–276.
- International Coffee Organization. Trade statistics tables. (2018). <http://www.ico.org/prices/po-production.pdf>/ Accessed 06.04.18.
- Kalaska, B., Piotrowski, L., Leszczynska, A., Michalowski, B., Kramkowski, K., Kaminski, T., ... Mogielnicki, A. (2014). Antithrombotic effects of pyridinium compounds formed from trigonelline upon coffee roasting. *Journal of Agricultural & Food Chemistry*, 62, 2853–2860.
- Kurzrock, T., & Speer, K. (2001). Diterpenes and diterpene esters in coffee. *Food Reviews International*, 17, 433–450.
- Ludwig, I. A., Clifford, M. N., Lean, M. E., Ashihara, H., & Crozier, A. (2014). Coffee: biochemistry and potential impact on health. *Food & Function*, 5, 1695–1717.
- Machado-Filho, J. A., Correia, A. O., Montenegro, A. B., Nobre, M. E., Cerqueira, G. S., Neves, K. R., ... Gs, D. B. V. (2014). Caffeine neuroprotective effects on 6-OHDA-lesioned rats are mediated by several factors, including pro-inflammatory cytokines and histone deacetylase inhibitions. *Behavioural Brain Research*, 264, 116–125.
- Miranda, A. M., Steluti, J., Fisberg, R. M., & Marchioni, D. M. (2017). Association between coffee consumption and its polyphenols with cardiovascular risk factors: A population-based study. *Nutrients*, 9, 276–290.
- Moenenard, M., Cortez, A., Machado, V., Costa, R., Luís, C., Coelho, P., ... Santos, A. (2016). Anti-angiogenic properties of cafestol and kahweol palmitate diterpene esters. *Journal of Cellular Biochemistry*, 117, 2748–2756.
- Moenenard, M., Erny, G. L., & Alves, A. (2016). Variability of some diterpene esters in coffee beverages as influenced by brewing procedures. *Journal of Food Science & Technology*, 53, 3916–3927.
- Moreira, A. S., Nunes, F. M., Domingues, M. R., & Coimbra, M. A. (2012). Coffee melanoidins: Structures, mechanisms of formation and potential health impacts. *Food & Function*, 3, 903–915.
- Muhammad, I., Takamatsua, S., Mustafaa, J., Khana, S. I., Khana, I. A., Samoylenkoa, V., ... Dunbara, D. C. (2007). COX-2 inhibitory activity of cafestol and analogs from coffee beans. *Natural Product Communications*, 3, 11–16.
- Muriel, P., & Arauz, J. (2010). Coffee and liver diseases. *Fitoterapia*, 81, 297–305.
- Naito, S., Yatagai, C., Maruyama, M., & Sumi, H. (2011). Effect of coffee extracts on plasma fibrinolysis and platelet aggregation. *Japanese Journal of Alcohol Studies & Drug Dependence*, 46, 260–269.
- Natella, F., Nardini, M., Belevi, F., Pignatelli, P., Di, S. S., Ghiselli, A., ... Scaccini, C. (2008). Effect of coffee drinking on platelets: Inhibition of aggregation and phenols incorporation. *British Journal of Nutrition*, 100, 1276–1282.
- Nehlig, A. (2016). Effects of coffee/caffeine on brain health and disease: What should I tell my patients? *Practical Neurology*, 16, 89–95.
- Nishimura, K., Hitotsuyanagi, Y., Sugeta, N., Sakakura, K. I., Fujita, K., Fukaya, H., ... He, D. H. (2006). Tricalysiolides A-F, new rearranged ent-kaurane diterpenes from *Tricalysia dubia*. *Tetrahedron*, 62, 1512–1519.
- Novaes, F. J. M., Oigman, S. S., Rezende, C. M., & Neto, F. R. D. A. (2015). New approaches on the analyses of thermolabile coffee diterpenes by gas chromatography and its relationship with cup quality. *Talanta*, 139, 159–166.
- Pan, M. H., Tung, Y. C., Yang, G., Li, S., & Ho, C. T. (2016). Molecular mechanisms of the anti-obesity effect of bioactive compounds in tea and coffee. *Food & Function*, 7, 4481–4491.
- Ranheim, T., & Halvorsen, B. (2005). Coffee consumption and human health—beneficial or detrimental? Mechanisms for effects of coffee consumption on different risk factors for cardiovascular disease and type 2 diabetes mellitus. *Molecular Nutrition & Food Research*, 49, 274.
- Ratnayake, W. M., Hollywood, R., O'Grady, E., & Stavric, B. (1993). Lipid content and composition of coffee brews prepared by different methods. *Food & Chemical Toxicology*, 31, 263–269.
- Saab, S., Mallam, D., Li, G. A. C., & Tong, M. J. (2014). Impact of coffee on liver diseases: A systematic review. *Liver International Official Journal of the International Association for the Study of the Liver*, 34, 495–504.
- Shen, Z., Dong, Z., Cheng, P., Li, L., Chen, Z., & Liu, J. (2003). Effects of plumbagin on platelet aggregation and platelet-neutrophil interactions. *Planta Medica*, 69, 605–609.
- Shen, C. P., Luo, J. G., Yang, M. H., & Kong, L. Y. (2015). Cafestol-type diterpenoids from the twigs of *Tricalysia fruticosa* with potential anti-inflammatory activity. *Journal of Natural Products*, 78, 1322–1329.
- Shu, Y., Liu, J. Q., Peng, X. R., Wan, L. S., Zhou, L., Zhang, T., & Qiu, M. H. (2014). Characterization of diterpenoid glucosides in roasted puer coffee beans. *Journal Agriculture and Food Chemistry*, 62, 2631–2637.
- Speer, K., & Speer, I. K. (2006). The lipid fraction of the coffee bean. *Brazilian Journal of Plant Physiology*, 18, 201–216.
- Tamaki, N., Matsunami, K., Otsuka, H., Shinzato, T., Aramoto, M., & Takeda, Y. (2008). Rearranged ent-kauranes from the stems of *Tricalysia dubia* and their biological activities. *Journal of Natural Medicines*, 62, 314–320.
- Urgert, R., Weg, G. V. D., Kosmeijerschuil, T. G., Bovenkamp, P. V. D., Hovenier, R., & Katan, M. B. (1995). Levels of the cholesterol-elevating diterpenes cafestol and kahweol in various coffee brews. *Journal of Agricultural & Food Chemistry*, 43, 2167–2172.
- Vitaglione, P., Fogliano, V., & Pellegrini, N. (2012). Coffee, colon function and colorectal cancer. *Food & Function*, 3, 916–922.
- Yin, H., Luo, J. G., & Kong, L. Y. (2013). Tetracyclic diterpenoids with isomerized isoprenoid skeleton and labdane diterpenoids from the fruits of *Amomum kravanh*. *Journal of Natural Products*, 76, 237–242.
- Zhao, H. X., Ren, H. L., Xu, X. L., Zhang, F. X., Ding, D. D., Yue, F. P., ... Zhong, W. K. (2014). Rapid screening for gutter oil adulteration in vegetable oil based on fatty acid methyl esters. *Food Science*, 35, 148–152.
- Zhou, J., Zhou, S., & Zeng, S. (2013). Experimental diabetes treated with trigonelline: Effect on β cell and pancreatic oxidative parameters. *Fundamental & Clinical Pharmacology*, 27, 279–287.